

## A Submicron InAlAs/n<sup>+</sup>-InP HFET with Reduced Impact Ionization

David R. Greenberg, Jesús A. del Alamo, and Rajaram Bhat\*

Massachusetts Institute of Technology, Cambridge, MA

\* Bellcore, Red Bank, NJ

### Abstract

We have fabricated submicron InAlAs/n<sup>+</sup>-InP HFETs that employ an InP channel layer to eliminate impact ionization and thus reduce gate leakage, decrease drain conductance, and improve breakdown voltage. Under typical bias conditions, our  $L_g = 0.8 \mu\text{m}$  devices achieve a low  $g_d$  of  $5.1 \text{ mS/mm}$ , leading to a voltage gain of 25, while gate current never exceeds  $17 \mu\text{A/mm}$ . This is approximately 60 times lower gate current than for typical InAlAs/InGaAs HEMTs, including edge-isolated devices. Off-state drain-source breakdown voltage is about 10 V at  $1 \text{ mA/mm}$  and increases as the device is turned on, confirming that impact ionization is negligible. Our results on a lattice-matched structure suggest considerable potential for optimization by using a strained insulator layer to reduce gate leakage and to improve breakdown still further.

### Introduction

InAlAs/InGaAs HFETs have shown promise as candidates for use in long wavelength optoelectronic receivers [1]. Despite their outstanding frequency response, however, InAlAs/InGaAs HFETs are vulnerable to impact ionization occurring at the drain end of the narrow bandgap channel even under normal biasing conditions [2]. This phenomenon brings down voltage gain ( $a_v$ ) through increased  $g_d$ , lowers the drain-source breakdown voltage ( $BV_{DS}$ ), and, in applications to optoelectronic receivers, degrades sensitivity through excess gate leakage noise [2-5]. Previous studies have explored the use of strained barrier layers to reduce the multiplication hole current into the gate [6-7] as well as the engineering of the cap layer over the drain-gate gap to lower the peak electric field in the drain [8]. The performance tradeoffs associated with these methods are still unclear.

To date, however, there has been little work exploring the use of the wide bandgap material InP rather than InGaAs as the channel layer in optoelectronic devices. InP is an attractive material for use in devices targeted at high-power telecommunications applications because of its exceptional breakdown field and high peak electron velocity. In addition, the existence of highly selective etchants for InGaAs and InAlAs over InP make InP an ideal etch-stop layer for use in recessed-gate and recessed-ohmic-contact fabrication processes. InP-channel HFETs have recently been demonstrated in both doped-channel [9] and modulation-doped [10] designs, achieving an excellent combination of high transconductance, current density, power density, and breakdown voltage.

This work examines the potential of submicron InAlAs/n<sup>+</sup>-InP HFETs for optoelectronic applications. In particular, we study the relative magnitude of impact ionization in this device structure. The heterostructure

design, first demonstrated in  $L_g \approx 2 \mu\text{m}$  devices in [9], relies on an InP layer as the active channel of the device. We find that the wide bandgap channel of InP eliminates any discernible impact ionization, resulting in low gate leakage current combined with low  $g_d$ , high  $a_v$ , and high  $BV_{DS}$ .

### Experiment

We have fabricated  $0.8 \mu\text{m} \times 200 \mu\text{m}$  devices using the MOCVD-grown heterostructure of Fig. 1. The heterostructure consists, from top to bottom, of a  $500 \text{ \AA}$   $\text{In}_{0.53}\text{Ga}_{0.47}\text{As}$  cap ( $N_D = 1 \times 10^{19} \text{ cm}^{-3}$ ), a  $50 \text{ \AA}$  undoped InP etch-stop layer, a  $250 \text{ \AA}$  undoped  $\text{In}_{0.52}\text{Al}_{0.48}\text{As}$  pseudoin insulator, a  $100 \text{ \AA}$  n<sup>+</sup>-InP channel ( $N_D = 5 \times 10^{18} \text{ cm}^{-3}$ ), a  $100 \text{ \AA}$  undoped InP subchannel, and a  $1000 \text{ \AA}$  undoped  $\text{In}_{0.52}\text{Al}_{0.48}\text{As}$  buffer/electron confinement layer grown on a S.I. InP substrate.

Fabrication begins with a mesa wet etch, followed by Ni/Au/Ge ohmic contact deposition, patterning, and rapid thermal annealing ( $390^\circ \text{C}$ , 15 s). After gate photolitho-

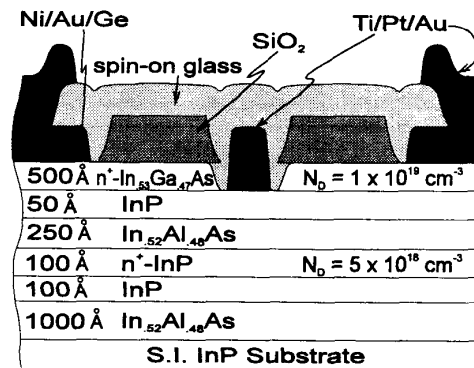


Figure 1: Schematic cross-section of the InAlAs/n<sup>+</sup>-InP HFET.

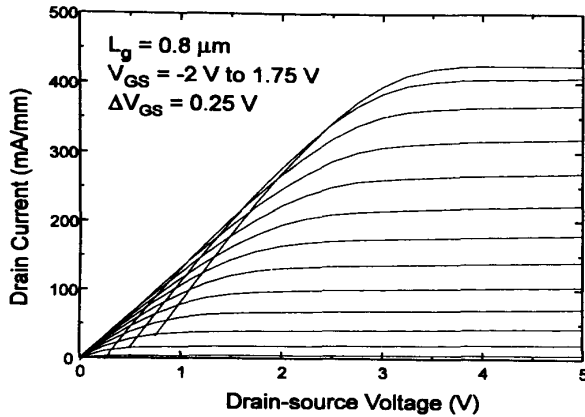


Figure 2:  $I_D$  vs.  $V_{DS}$  for an  $L_g = 0.8 \mu m$  device ( $V_{GS} = -2$  V to 1.75 V).

graphy, the  $n^+$ -InGaAs cap is selectively etched down to the InP etch-stop layer with 1:10:220  $H_2SO_4:H_2O_2:H_2O$  etchant just prior to the deposition and lift-off of Ti/Pt/Au gates. Precise timing of the etch or iterative monitoring of  $I_D$  is obviated by the better than 300:1 selectivity of this etchant for InGaAs on InP, which we have verified in etch tests. The resulting increased reliability and threshold voltage control is essential for circuit fabrication. Finally, we conclude fabrication with spin-on glass intermetal dielectric deposition and patterning (necessary for making circuits) followed by Ti/Pt/Au pad/second-level metal formation.

### Results and Discussion

Figs. 2 and 3 show  $I_D$  and  $g_m$  for a typical device (4.8  $\mu m$  source-drain spacing). Peak extrinsic and intrinsic values of  $g_m$  are typically 200  $mS/mm$  and 370  $mS/mm$ , respectively, for  $V_{DS} \geq 4$  V. The thin, heavily-doped channel and the use of an undoped insulator result in  $g_m$  with less than 10% frequency dispersion from DC to 3 GHz and sustained over a broad  $V_{GS}$  swing, contributing to a large typical maximum

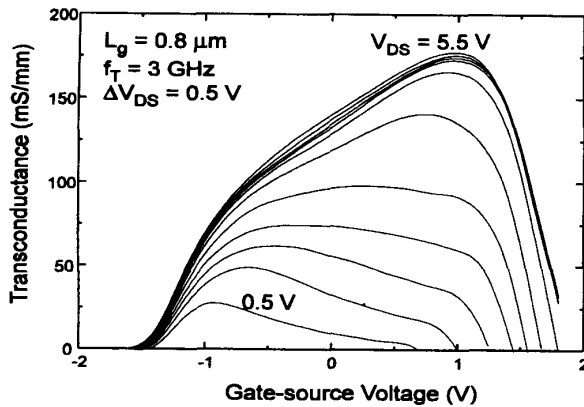


Figure 3:  $g_m$  vs.  $V_{GS}$  for an  $L_g = 0.8 \mu m$  device ( $V_{DS} = 0.5$  V to 5.5 V).

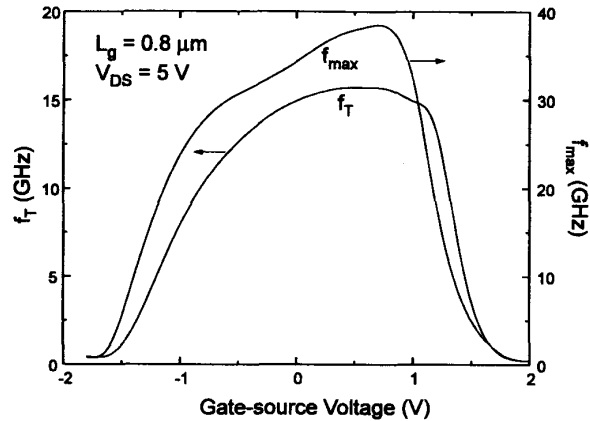


Figure 4:  $f_T$  and  $f_{max}$  vs.  $V_{GS}$  for an  $L_g = 0.8 \mu m$  device ( $V_{DS} = 5$  V).

drain current of 450  $mA/mm$ . Fig. 4 shows the behavior of  $f_T$  and  $f_{max}$  vs.  $V_{GS}$ , with  $f_T$  and  $f_{max}$  achieving peak values of 15 GHz and 38 GHz, respectively. We have examined the scaling behavior of  $g_{m0}$  and  $f_T$  with  $L_g$  in the range between 0.6  $\mu m$  and 5  $\mu m$ . We find that our devices are governed by mobility-limited transport for  $L_g > 1.8 \mu m$  and by velocity-saturation-limited transport for shorter gate lengths. Specifically, we extract a channel electron mobility of 1750  $cm^2/V\cdot s$  and a saturation velocity of  $1 \times 10^7$   $cm/s$ .

Since low gate leakage is particularly important in high sensitivity optoelectronic receivers, we plot  $I_G$  vs.  $V_{GS}$  for several values of  $V_{DS}$  for a typical device in Fig. 5. Despite the low  $\Delta E_c$  (0.27 eV - 0.39 eV [11,12]) of the InAlAs/InP system, we find that  $|I_G|$  remains less than 17  $\mu A/mm$  in the useful  $V_{GS}$  range between -1 V and 1 V, at a typical  $V_{DS}$  of 4 V. This value is almost 60 times lower than for reported lattice-matched InGaAs HEMTs operated at a lower  $V_{DS}$  of 2 V (including devices with edge isolation) [6,7,13,14]. Significantly, the curves also lack the characteristic negative

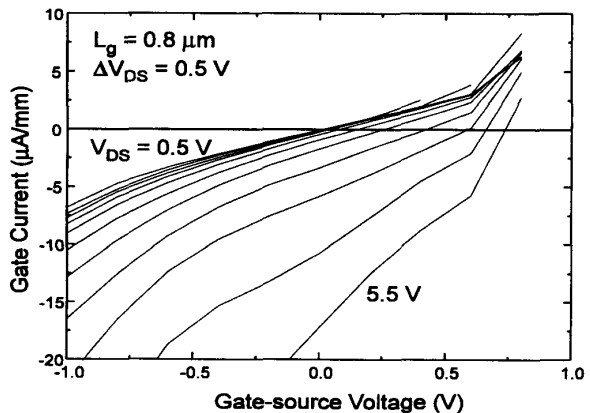


Figure 5:  $I_G$  vs.  $V_{GS}$  for an  $L_g = 0.8 \mu m$  device ( $V_{DS} = 0.5$  V to 5.5 V).

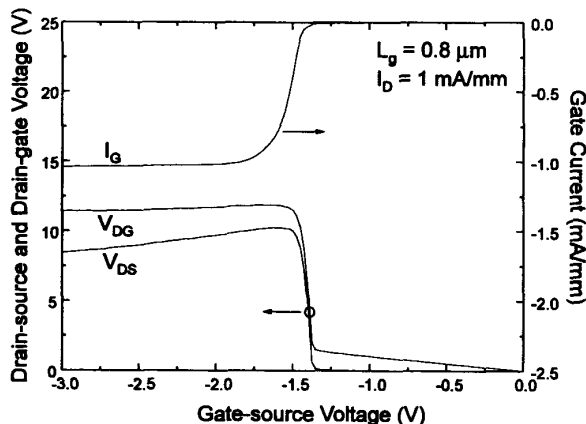


Figure 6:  $V_{DS}$ ,  $V_{DG}$ , and  $I_G$  vs.  $V_{GS}$  at  $I_D = 1 \text{ mA/mm}$  for an  $L_g = 0.8 \mu\text{m}$  device.

hump in  $I_G$  which is the signature of impact ionization [6,7,13,14], proving that these devices are indeed completely free of this deleterious effect.

The behavior of drain-source and drain-gate breakdown voltage is another test for the presence of impact ionization. In Fig. 6, we plot both  $V_{DS}$ ,  $V_{DG}$ , and  $I_G$  vs.  $V_{GS}$  at  $I_D = 1 \text{ mA/mm}$  using the Drain-Current Injection technique described by Bahl [15]. This figure indicates drain-source and drain-gate breakdown voltages ( $BV_{DS}$  and  $BV_{DG}$ ) of 10 V and 12 V, respectively. The fact that breakdown in our device occurs at constant  $V_{DG}$  means that breakdown is gate-drain limited. This behavior, and the values of  $BV_{DS}$  and  $BV_{DG}$ , do not depend on gate length in the examined range from 0.8  $\mu\text{m}$  to 2  $\mu\text{m}$  (within statistical variation).

The role of impact ionization in breakdown is best studied by examining the  $I_D$  dependence of the three-terminal drain-source breakdown voltage as the device is turned on. We plot  $I_D$  vs.  $V_{DS}$  in Fig. 7 for a typical device as  $V_{GS}$  is

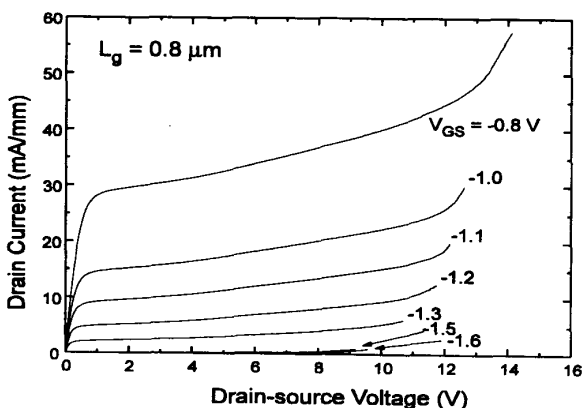


Figure 7:  $I_D$  vs.  $V_{DS}$  for an  $L_g = 0.8 \mu\text{m}$  device showing  $I_D$  dependence of drain-source breakdown above threshold.

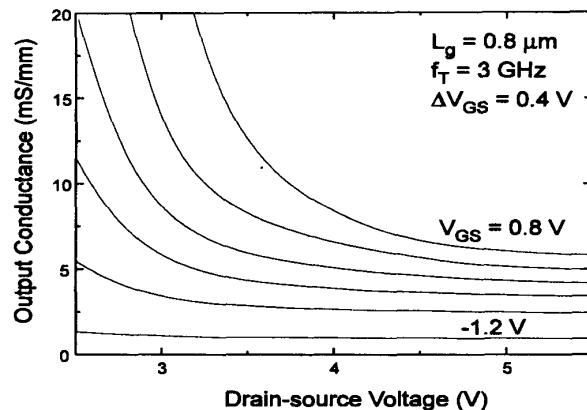


Figure 8:  $g_d$  vs.  $V_{DS}$  for an  $L_g = 0.8 \mu\text{m}$  device ( $V_{GS} = -1.2 \text{ V}$  to 0.8 V).

varied from just below to moderately above threshold. Since  $I_D$  increases with increasing  $V_{GS}$ , the drain-source breakdown voltage should degrade with rising  $V_{GS}$  if it involves impact ionization in the channel. Instead, the breakdown voltage *improves* as the device is turned on, contrary to the behavior of InAlAs/InGaAs HFETs and indicating that channel impact ionization is negligible. This behavior is consistent with breakdown being set by thermionic field-emission of electrons from the gate, over the insulator, and into the channel. As a result of low impact ionization and the thin-channel design, our devices display very low  $g_d$  as illustrated in Fig. 8 (for 3 GHz). This yields good values for  $a_v$ , despite only modest values for  $g_m$ . At a typical bias of  $V_{GS} = 0 \text{ V}$  and  $V_{DS} = 4 \text{ V}$ , for example, our devices simultaneously achieve  $g_m = 133 \text{ mS/mm}$ ,  $g_d = 5.1 \text{ mS/mm}$ ,  $a_v = 26$ , and  $I_G = 3.3 \mu\text{A/mm}$ . At this bias, our devices also achieve an  $f_T$  of 12 GHz and an  $f_{max}$  of 35 GHz, sufficient for multigigabit applications. Additionally, pulse measurements show less than 5% gate and drain lag.

## Conclusion

In summary, we have fabricated submicron InAlAs/ $n^+$ -InP HFETs which, by virtue of their InP channel layer, are completely free of impact ionization. The absence of impact ionization results in very low  $I_G$  (and thus potentially low input noise in optoelectronic receiver applications), low  $g_d$ , excellent voltage gain, and high breakdown voltage. Our results on a lattice-matched structure suggest great potential for optimization by using a strained insulator layer to reduce gate leakage and to improve breakdown still further.

## Acknowledgements

This work was made possible through grants DL-H-441694 and DL-H-441638 from C.S. Draper Laboratory as well as through equipment grants from Bellcore and Hewlett Packard. In addition, DRG received personal fellowship support from the Fannie and John Hertz Foundation.

### References

1. W.P. Hong, G.K. Chang, R. Bhat, J.L. Gimlett, C. Nguyen, G. Sasaki, and M. Koza, "High performance InAlAs/InGaAs MSM-HEMT receiver OEIC grown by OMCVD on patterned InP substrates," *Electron. Lett.*, vol. 25, p. 1561, 1989.
2. G.G. Zhou, A. Fisher-Colbrie, J. Miller, Y.C. Pao, B. Hughes, L. Studebaker, and J.S. Harris, Jr., "High output conductance of InAlAs/InGaAs/InP MODFETs due to weak impact ionization in the InGaAs channel," *IEDM Tech. Digest*, p. 247, 1991.
3. S.R. Bahl and J.A. del Alamo, "Physics of breakdown of InAlAs/n<sup>+</sup>-InGaAs heterostructure field-effect transistors," *Proc. 5<sup>th</sup> Int. Conf. on InP and Rel. Mat.*, Paris (France), p. 243, 1993.
4. D.J. Newson, R.P. Merrett, and B.K. Ridley, "Influence of Domain Formation on the  $V_{ds}$  dependence of noise and gate leakage in InGaAs FETs," *Proc. 3<sup>rd</sup> Int. Conf. on InP and Re. Mat.*, Cardiff, Wales (U.K.), p. 427, 1991.
5. J. Dickmann, S. Schildberg, H. Dämbkes, S.R. Bahl, and J.A. del Alamo, "Characterization of the breakdown behavior of pseudomorphic InAlAs/InGaAs/InP HEMTs with high breakdown voltages," *20<sup>th</sup> Int. Symp. on GaAs and Rel. Comp.*, Freiburg (Germany). To be published.
6. C. Heedt, F. Buchali, W. Prost, D. Fritzsche, H. Nickel, and F.J. Tegude, "Extremely low gate leakage InAlAs/InGaAs HEMT," *Int. Symp. on GaAs and Rel. Comp.*, Karuizawa (Japan), 1992. *Institute of Physics Conference Series*, no. 129, p. 941, 1993.
7. C. Heedt, F. Buchali, W. Prost, D. Fritzsche, H. Nickel, and F.J. Tegude, "Characterization of impact ionization in InAlAs/InGaAs/InP HEMT structures using a novel photocurrent-measurement technique," *Proc. 5<sup>th</sup> Int. Conf. on InP and Rel. Mat.*, Paris (France), p. 247, 1993.
8. Y.C. Pao and J.S. Harris Jr., "Low-conductance drain (LCD) design of InAlAs/InGaAs/InP HEMT's," *IEEE Electron Dev. Lett.*, vol. 13, no. 10, p. 535, 1992.
9. D.R. Greenberg, J.A. del Alamo, and R. Bhat, "A recessed-gate InAlAs/n<sup>+</sup>-InP HFET with an InP etch-stop layer," *IEEE Electron Dev. Lett.*, vol. 13, no. 3, p. 137, 1992.
10. O. Aina, M. Burgess, M. Mattingly, A. Meerschaert, J.M. O'Connor, M. Tong, A. Ketterson, and I. Adesida, "A 1.45 W/mm, 30 GHz InP-channel power HEMT," *IEEE Electron Dev. Lett.*, vol. 13, no. 5, p.300, 1992.
11. L. Aina, M. Mattingly, and L. Stecker, "Photoluminescence from AlInAs/InP quantum wells grown by organo-metallic vapor phase epitaxy," *Applied Phys. Lett.*, vol. 53, no. 17, p. 1620, 1988.
12. J.R. Waldrop, E.A. Kraut, C.W. Farley, and R.W. Grant, "Measurement of AlAs/InP and InP/In<sub>0.52</sub>Al<sub>0.48</sub>As heterojunction band offsets by x-ray photoemission spectroscopy," *J. Vac. Sci. Technol. B*, vol. 8, p. 768, 1990.
13. F. Buchali, C. Heedt, W. Prost, I. Gyuro, and F.J. Tegude, "Analysis of gate leakage on MOVPE grown InAlAs/InGaAs/InP HFETs," *Microelectronic Engineering*, vol. 19, p. 401, 1992.
14. A.A. Moolji, "Impact Ionization in InAlAs/InGaAs HFETs," *B.S. Thesis*, M.I.T., Cambridge, MA., June, 1993.
15. S.R. Bahl and J.A. del Alamo, "A new drain-current injection technique for the measurement of off-state breakdown voltage in FET's," *IEEE Trans. Electron Dev.*, vol. 40, no. 8, p. 1558, 1993.